Biochemical Pharmacology 83 (2012) 574–585

Contents lists available at SciVerse ScienceDirect

Biochemical Pharmacology

journal homepage: www.elsevier.com/locate/biochempharm

Homologous recombination repair-dependent cytotoxicity of the benzotriazine di-*N*-oxide CEN-209: Comparison with other hypoxia-activated prodrugs

Francis W. Hunter [a], Jingli Wang [a], Rita Patel [a], Huai-Ling Hsu [a], Anthony J.R. Hickey [b], Michael P. Hay [a], William R. Wilson [a,*]

[a] Auckland Cancer Society Research Centre, University of Auckland, Private Bag 92019, Auckland, New Zealand
[b] School of Biological Sciences, University of Auckland, Private Bag 92019, Auckland, New Zealand

ARTICLE INFO

Article history:
Received 6 October 2011
Accepted 1 December 2011
Available online 13 December 2011

Keywords:
Hypoxia-activated prodrug
Homologous recombination repair
Redox cycling
CEN-209
Tirapazamine
TH-302

ABSTRACT

CEN-209 (SN30000) is a second-generation benzotriazine di-*N*-oxide currently in advanced preclinical development as a hypoxia-activated prodrug (HAP). Herein we describe the DNA repair-, hypoxia- and one-electron reductase-dependence of CEN-209 cytotoxicity. We deployed mutant CHO cell lines to generate DNA repair profiles for CEN-209, and compared the profiles with those for other HAPs. Hypoxic selectivity of CEN-209 was significantly greater than PR-104A and the nitro-chloromethylbenzindoline (nCBI/SN29428) and comparable to tirapazamine and TH-302. CEN-209 was selective for homologous recombination (HR) repair-deficient cells (*Rad51d*$^{-/-}$), but less so than nitrogen mustard prodrugs TH-302 and PR-104A. Further, DNA repair profiles for CEN-209 differed under oxic and hypoxic conditions, with oxic cytotoxicity more dependent on HR. This feature was conserved across all three members of the benzotriazine di-*N*-oxide class examined (tirapazamine, CEN-209 and CEN-309/SN29751). Enhancing one-electron reduction of CEN-209 by forced expression of a soluble form of NADPH:cytochrome P450 oxidoreductase (sPOR) increased CEN-209 cytotoxicity more markedly under oxic than hypoxic conditions. Comparison of oxygen consumption, H_2O_2 production and metabolism of CEN-209 to the corresponding 1-oxide and nor-oxide reduced metabolites suggested that enhanced oxic cytotoxicity in cells with high one-electron reductase activity is due to futile redox cycling. This study supports the hypothesis that both oxic and hypoxic cell killing by CEN-209 is mechanistically analogous to tirapazamine and is dependent on oxidative DNA damage repaired via multiple pathways. However, HAPs that generate DNA interstrand cross-links, such as TH-302 and PR-104, may be more suitable than benzotriazine di-*N*-oxides for exploiting reported HR repair defects in hypoxic tumour cells.

1. Introduction

Pathological hypoxia, which arises through dysfunction of tumour vasculature, is a potential limiting factor for all major cancer treatment modalities and at the same time an attractive target because it is more severe in tumours than normal tissues [1–3]. A number of strategies for exploiting tumour hypoxia are now in clinical or preclinical development, with the majority employing relatively inert prodrugs that undergo selective one-electron reduction under hypoxia to release DNA-reactive cytotoxins [3,4]. Hypoxia-activated prodrugs (HAPs) currently in development include the dinitrobenzamide mustard PR-104 (a phosphate pre-prodrug of PR-104A) [5], the nitroimidazole mustard TH-302 [6], and nitro derivatives of the duocarmycin class of DNA minor groove alkylators such as the nitro-chloromethylbenzindoline (nCBI) SN29428 [7] (see Table 1 for structures). PR-104 and TH-302, both currently undergoing clinical evaluation, are thought to act primarily by hypoxia-selective release of potent DNA cross-linking metabolites [8,9].

The most thoroughly investigated HAP is tirapazamine (TPZ), a benzotriazine di-*N*-oxide that undergoes oxygen-inhibited reduction to reactive free radicals [10,11] which induce oxidative DNA damage [12–14]. TPZ showed promising indications of activity in early clinical trials [15,16] but did not extend overall survival in combination with cisplatin and radiotherapy for advanced head and neck cancers in a recent phase III study [17]. Besides the lack of selection for patients with hypoxic tumours [18] and sub-optimal radiotherapy in the latter study [19], another factor likely to have contributed to the failure of TPZ is that metabolic consumption of the prodrug during diffusion prevents it accessing the most severely hypoxic cells in sufficient concentrations to exert optimal therapeutic effects [20]. To address this problem, we recently identified CEN-209 (SN30000) as an improved second-generation TPZ analogue,

* Corresponding author. Tel.: +64 9 923 6883; fax: +64 9 373 7571.
E-mail address: wr.wilson@auckland.ac.nz (W.R. Wilson).

0006-2952/$ – see front matter © 2011 Published by Elsevier Inc.
doi:10.1016/j.bcp.2011.12.005

Table 1
Hypoxia-activated prodrugs, effector cytotoxins and reference compounds used in this study. Chemical classes, proposed mechanism of action and active cytotoxins (where investigated) for each prodrug are indicated. Chemical structures for the five prodrugs are show below.

Prodrug	Chemical class	Active cytotoxin	DNA lesions
Tirapazamine	Benzotriazine di-*N*-oxide	–	Oxidative DNA damage
CEN-209 (SN30000)	Benzotriazine di-*N*-oxide	–	Oxidative DNA damage[a]
TH-302	2-Nitroimidazole mustard	Mechlorethamine[b]	DNA cross-linking
PR-104A	Dinitrobenzamide mustard	PR-104H, chlorambucil[b]	DNA cross-linking
nCBI (SN29428)	Nitro-chloromethylbenzindoline	aCBI	Minor groove alkylation

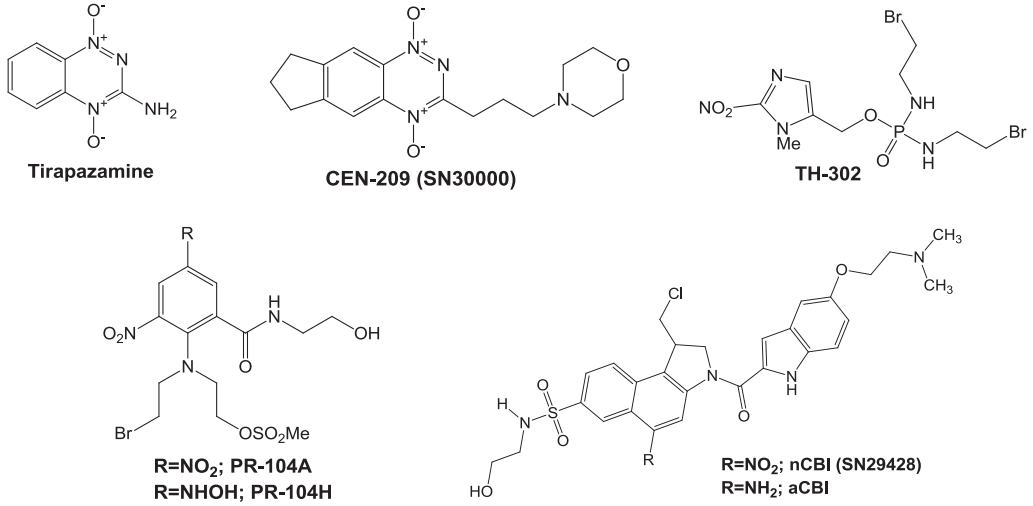

[a] By analogy with tirapazamine.
[b] Mechlorethamine and chlorambucil are close analogues of the active metabolites of TH-302 and PR-104A, respectively, and were used as reference compounds in that context.

using a spatially-resolved pharmacokinetic/pharmacodynamic model that explicitly considers extravascular transport during lead optimisation [21]. CEN-209 showed a higher diffusion coefficient than TPZ in multicellular layer cultures, indicating superior tissue penetration properties, and higher hypoxic selectivity and potency in tissue culture along with improved activity in xenograft models. CEN-209 is scheduled to begin phase I clinical evaluation through Centella Therapeutics and Cancer Research UK in 2012.

Recent studies highlight a potentially important determinant of sensitivity to HAPs that generate DNA-reactive metabolites as their cytotoxic effectors. The homologous recombination (HR) repair pathway, required for error-free resolution of DNA double-strand breaks, has a central role in the repair of most replication-associated lesions induced by chemotherapy [22]. As a consequence cells deficient in HR, such as those harbouring mutations in the breast cancer susceptibility genes *BRCA1* and *BRCA2*, are hypersensitive to compounds that damage DNA replication forks [23]. This is of particular interest in the context of clinical development of HAPs because chronic hypoxia itself suppresses HR repair by down-regulating expression of key HR proteins including BRCA1 and RAD51 [24–26] with attendant increases in sensitivity to radiation and DNA-damaging cytotoxins [25]. Simultaneously targeting hypoxia and loss of HR may therefore provide an avenue for enhancing the therapeutic index of HAPs. Selectivity for HR deficiency under hypoxia in various cellular models has been described for TPZ [27], PR-104A [9], and TH-302 [28]. However, no such study has been undertaken for CEN-209 and no quantitative comparison of the potential for HAPs across different chemical classes to exploit HR defects has been reported.

In the present study we deploy well-characterised CHO cell lines with loss-of function mutations in the HR (*Rad51d*), base excision repair (*Xrcc1*), nucleotide excision repair (*Ercc1*, *Xpf*, *Ercc2*), non-homologous end joining (*Prkdc*) and Fanconi anaemia (*FancG*) pathways to describe the dependence of CEN-209 cytotoxicity on DNA repair in oxic and hypoxic cells and compare this with TPZ, TH-302, PR-104A and nCBI. We performed short term drug exposures under oxia and hypoxia to isolate the prodrug activation component of HAP sensitivity independent of down-regulation of HR repair and other changes in cellular phenotype that occur in chronically hypoxic cells. We demonstrate that CEN-209 shares a common mechanism of action with TPZ but that these benzotriazine-di-*N*-oxides are less dependent on HR repair than the nitrogen mustard chemotypes, particularly under hypoxia. By relating cytotoxicity of CEN-209 to its bioreductive metabolism, we present evidence that the mechanisms of cell killing by CEN-209 differ under oxic and hypoxic conditions, in cells with high one-electron reductase activity, as a result of futile redox cycling in the presence of oxygen.

2. Methods

2.1. Compounds

TPZ [29], CEN-209 [30], CEN-309 (SN29751) [31], TH-302 [6], mechlorethamine [32], PR-104A [33], PR-104H [9], nCBI [7] and aCBI [7] were synthesised at the Auckland Cancer Society Research Centre as reported. Chlorambucil was purchased from Sigma–Aldrich. All compounds were confirmed for >95% purity by HPLC and stored as stock solutions in saline (CEN-209, CEN-309), acetonitrile (Merck; PR-104H), 0.1 N HCl (mechlorethamine) or DMSO (Merck; all others) at −80 °C.

2.2. Cell lines

Cell lines were maintained in alpha minimal essential medium (αMEM, Invitrogen) with 5% foetal calf serum (FCS; Moregate

Biotech, New Zealand), 100 units/mL penicillin and 100 μg/mL streptomycin (both from Invitrogen). All cell lines were cultured for less than 2 months from frozen stocks confirmed to be *Mycoplasma*-negative by PCR-ELISA (Roche Diagnostics). The Chinese hamster ovary (CHO) cell lines used and their origins and genotypes were as follows: AA8 (wild type [34]), 51D1 (*Rad51d* homozygous knockout generated from AA8 [35], identified herein as $51D^{-/-}$), 51D1.3 (51D1 complemented with full-length Chinese hamster *Rad51d* [35], identified herein as $51D^{+/+}$), EM9 (*Xrcc1* mutant [36]), UV4 (*Ercc1* mutant [37,38], UV41 (*Xpf* mutant [37,39,40]), 41cER4.40.1 (UV41 complemented with human *Xpf* [40]), UV5 (*Ercc2* mutant [41]), V3 (mutated in the gene for DNA-PKcs, *Prkdc* [42]), and KO40 (*FancG* null [43]). For simplicity these cell lines are identified in this manuscript by genotype. The generation of soluble NADPH:cytochrome P450 oxidoreductase (sPOR) over-expressing $51D^{-/-}$ sPOR and $51D^{+/+}$ sPOR cell lines has been described [9].

2.3. Cytotoxicity assays

In vitro drug sensitivity was evaluated by IC_{50} assay. Cells were seeded in 96-well plates at a density of 400 or 800 cells/0.1 mL (electronic particle counter, Beckman Coulter) and exposed to varying concentrations of compounds for 4 h under aerobic or hypoxic conditions as described elsewhere [44]. Media for drug incubations was αMEM containing 10% FCS, 200 μM 2′-deoxycytidine (Sigma–Aldrich), and D-glucose (Nuclear Supplies) supplemented to 17 mM. Hypoxic incubations were performed in a H_2/Pd catalyst-scrubbed anaerobic chamber (Coy Laboratory Products) with media and consumables pre-equilibrated for >3 days to remove residual oxygen. Cells were reoxygenated immediately after drug treatment and cultured for 4 days in CO_2 incubators prior to staining with sulphorhodamine B (Sigma–Aldrich) to quantitate cell density [45]. IC_{50} values were calculated, using 4 parameter logistic regression, as the drug concentration reducing staining to 50% of untreated controls on the same plate. Hypoxic cytotoxicity ratio (HCR) was defined as (IC_{50} oxic)/(IC_{50} hypoxic). Hypersensitivity factor (HF) for DNA repair pathway mutants was defined as (IC_{50} repair proficient reference line)/(IC_{50} repair-defective line). Reference cell lines corresponding to each repair-defective line are specified in supplementary Tables S1 and S2. All ratios (HCR and HF) are intra-experiment comparisons.

2.4. Rad51 immunofluorescence

Cells were seeded on sterile poly-D-lysine-coated glass coverslips (BD Biosciences) in 6-well plates and incubated overnight, then treated with 8 Gy ionising radiation (IR; Eldorado model G ^{60}Co radiotherapy machine) or mock irradiated and incubated for 8 h before fixation in 2% paraformaldehyde (Sigma–Aldrich). Cells were rehydrated in ice-cold PBS, permeabilised in 0.25% Triton X-100 (Sigma–Aldrich) in PBS for 20 min and blocked using 5% goat serum (Invitrogen) in 0.1% PSB–Tween 20 (Global Science) for 30 min at room temperature. The specimens were then probed with anti-RAD51 primary antibody (rabbit polyclonal ab63801, Abcam) diluted 1:1000 in blocking buffer for 1 h at room temperature. The coverslips were washed thoroughly in PBS and probed with Cy3-conjugated goat anti-rabbit secondary antibody (Invitrogen) diluted 1:500 in blocking buffer for 30 min in the dark at room temperature. Cells were counterstained with 2.5 μg/mL 4′,6-diamidino-2-phenylindole (DAPI, Sigma–Aldrich) for 1 min and mounted on glass microscope slides using ProLong Gold (Invitrogen). Slides were air dried before storing at 4 °C. Images were captured using a Leica DMR microscope with Nikon Digital Sight DS-U1 camera and 100× objective lens. Nuclei presenting ≥1 Rad51 focus were scored as positive by manual counting. Typically, >150 random nuclei per slide were scored within replicate experiments.

2.5. Cell cycle analysis

Exponential phase monolayer cultures, established in parallel to Rad51 immunofluorescence specimens, were irradiated with 8 Gy IR or mock irradiated and incubated for 8 h prior to fixation in 70% ethanol. Cells were stained with 1 μg/mL DAPI in 0.1% PBS–Tween 20 at room temperature for 30 min. Cellular fluorescence was measured using a Becton Dickinson FACScan flow cytometer and cell cycle analysis performed in ModFit LT 3.2 (Verity Software House).

2.6. Western blot analysis

For POR immunoblotting, cellular lysates were harvested in radioimmunoprecipitation assay buffer and protein concentration determined by bicinchoninic acid (BCA; Sigma–Aldrich) assay. Thirty micrograms of protein was loaded on 4–12% gradient SDS-PAGE gels, transferred, blocked, probed with anti-POR (mouse monoclonal sc25263, Santa Cruz Biotechnology) or anti-actin (mouse monoclonal MAB1501R, Chemicon) primary antibodies at 1:5000 dilution, and imaged using chemiluminescent ECL detection (Thermoscientific).

2.7. POR enzyme activity

POR reductase activity in cellular S-9 fractions was determined by spectrophotometric assay as cyanide-resistant, NADPH-dependent reduction of cytochrome c as described elsewhere [46]. Total protein in S-9 fractions was measured by BCA assay.

2.8. Liquid chromatography–tandem mass spectrometry (LC–MS/MS) assay of CEN-209 metabolism

In vitro cellular metabolism of CEN-209 was assayed by LC–MS/MS as detailed elsewhere [47]. Briefly, exponentially growing cells were harvested in trypsin/EDTA, counted, and resuspended in αMEM containing 5% FCS, 200 μM 2′-deoxycytidine and 17 mM D-glucose in 96-well plates. CEN-209 diluted in medium was added to wells containing 10^4 or 10^5 cells and the plates incubated under oxia or hypoxia for 3 h. After incubation the plates were placed on ice, the medium collected, and ice-cold methanol containing octadeuterated ($^8H_2$-morpholino) versions of CEN-209 and its metabolites (nor-oxide and 1-oxide) as internal standards was added to each well. The methanol extracts were combined with the removed medium and stored at −80 °C until LC–MS/MS analysis. CEN-209 and its 1-oxide and nor-oxide metabolites were quantified using an Agilent 6460 triple quadrupole mass spectrometer with ultra high pressure liquid chromatography and electrospray ionisation interface in positive ion mode.

2.9. Non-respiratory oxygen consumption and net H_2O_2 formation

Cellular oxygen consumption and net H_2O_2 formation rates were measured simultaneously using OROBOROS® O2K oxygraphs (Anton Paar, Graz, Austria) incorporating purpose-built fluorospectrometers mounted against the viewing port of each chamber [48]. These systems utilise 520 nm light emitting diodes (LEDs) mounted in black acetate blocks in front of the chamber window, and an adjacent photodiode with a 590 nm low pass filter. Measurements were performed at 37 °C with 2 mL chamber volumes containing DMEM + 5% FCS, initially at air saturation (186.1 μM at 101.3 kPa barometric pressure). Cells (1×10^6, grown as stirred single-cell suspensions in spinner flasks) were added to each chamber, with superoxide dismutase (10 U), horseradish peroxidase (10 U), and Amplex UltraRed (50 μM, all from Molecular Probes Invitrogen) and endogenous respiration

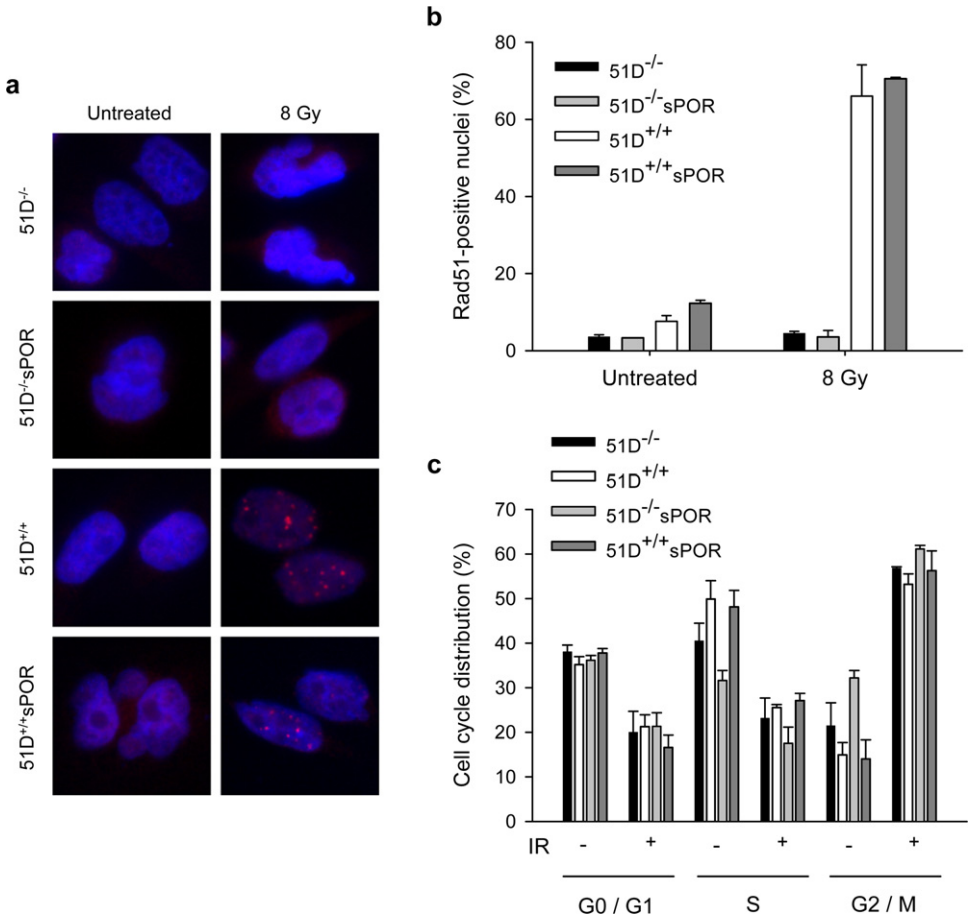

Fig. 1. Rad51 focus formation and cell cycle distribution 8 h after irradiation (8 Gy) of $51D^{+/+}$, $51D^{-/-}$ and sPOR cells. (a) Example micrographs showing fluorescent Rad51 (red) and nuclear (DAPI, blue) staining by immunocytochemistry. (b) The fraction of cells positive for Rad51 foci in irradiated and untreated cultures. (c) Cell cycle distribution at the time of Rad51 focus assays was determined by flow cytometry in parallel irradiated (8 Gy) and untreated cultures. Values are inter-experiment means and errors are SEM for 2 experiments. (For interpretation of the references to colour in this figure legend, the reader is referred to the web version of the article.)

flux rates allowed to reach steady states. Rotenone (1 nmol) was then added and CEN-209 (50 mM stock in saline) titrated stepwise at intervals of ~5 min. Fluorescence (oxidation of Amplex UltraRed by horseradish peroxidase/H_2O_2, calibrated with H_2O_2 standards) and polarographic signals were integrated in DATLAB 4.3.

2.10. Statistics

All histograms show inter-experiment means plus SEM derived from multiple independent experiments. Statistical significance was determined using Student's two-tailed *t*-test for comparison of two groups and ANOVA/Holm–Sidak for comparison between multiple groups. * denotes $P < 0.05$, ** denotes $P < 0.01$.

3. Results

3.1. Characterisation of HR phenotype in Rad51d null CHO cells

As a model for HR-deficient cancer cells we deployed a CHO cell line with genetic deletion of the Rad51 paralogue *Rad51d*, and an isogenic control line complemented with Chinese hamster *Rad51d* ($51D^{-/-}$ and $51D^{+/+}$ cells, respectively), a protein reported to be critical for HR [35]. In addition, we previously generated stable clones expressing a soluble, N-terminal membrane anchor-truncated, form of the one-electron reductase NADPH:cytochrome P450 oxidoreductase (sPOR; see Section 3.4) in both $51D^{-/-}$ and $51D^{+/+}$ genetic backgrounds [9]. To confirm the HR phenotype in these cell lines we measured IR-induced nuclear Rad51 foci 8 h after irradiation (Fig. 1a). In contrast to $51D^{+/+}$ cells, $51D^{-/-}$ cells demonstrated complete absence of Rad51 foci in response to IR (Fig. 1b). There was a small increase in baseline Rad51 foci associated with expression of sPOR in $51D^{+/+}$ cells, but sPOR did not affect induction of Rad51 foci in response to irradiation of these cells. As HR is suppressed in G0/G1-phase cells [49], we performed cell cycle analysis in parallel cultures to exclude differences in proliferation as a potential confounding variable for HR status. There was no significant difference in the fraction of cells in G0/G1 phases across the four cell lines in either irradiated or unirradiated cultures at the time of the focus formation assays ($P > 0.05$; Fig. 1c). These results also demonstrated that IR-induced G2-phase arrest is retained in the HR-defective cell lines.

3.2. Hypersensitivity to CEN-209 and reference compounds in HR-deficient cells

To evaluate the role of HR in repairing DNA lesions induced by CEN-209, and to compare candidate compounds for exploiting HR defects in hypoxic cells more generally, we challenged $51D^{+/+}$ and $51D^{-/-}$ cells with CEN-209 and the reference prodrugs and cytotoxins listed in Table 1 by IC_{50} assay under oxic and hypoxic conditions. The absolute IC_{50} values are provided in supplementary Table S1, and intra-experiment IC_{50} ratios for hypoxic selectivity (hypoxic cytotoxicity ratio) and HR deficiency (hypersensitivity factor) are shown in Fig. 2. CEN-209 was highly selective for hypoxia in repair-proficient cells, with an HCR for $51D^{+/+}$ cells of 280 which was approximately 30-fold greater than PR-104A and

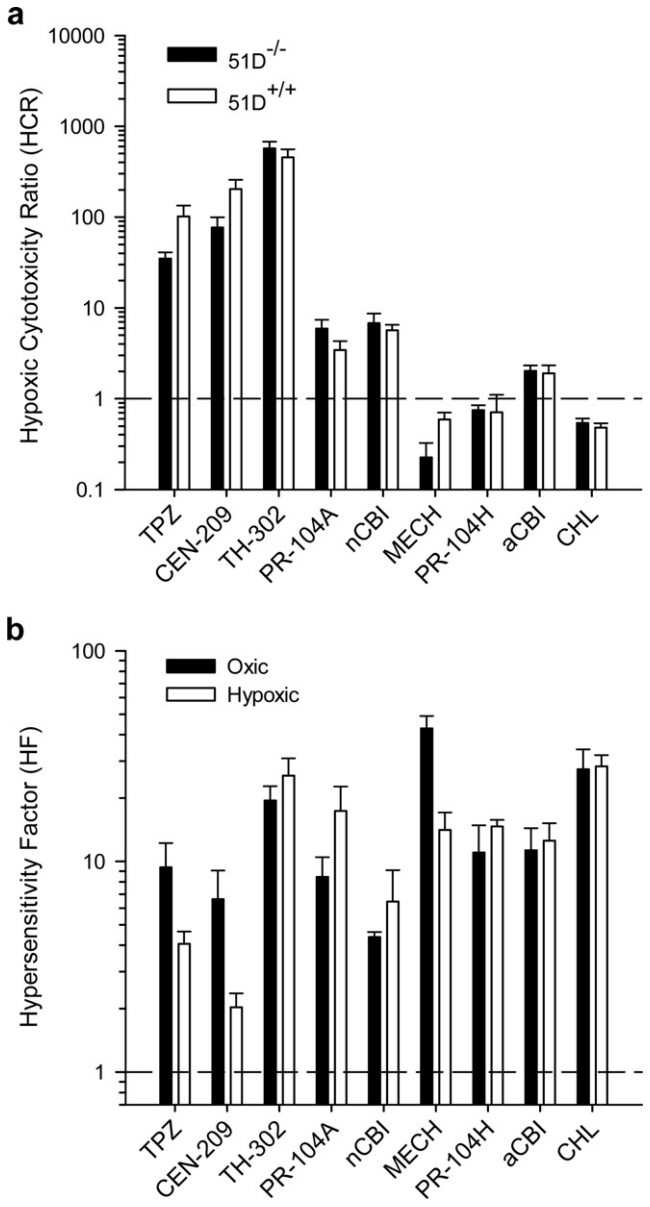

Fig. 2. Hypoxia- and HR-dependence of inhibition of cell growth measured 4 days after 4 h exposure to prodrugs and reference cytotoxins. (a) Hypoxic selectivity of compounds in $51D^{-/-}$ and $51D^{+/+}$ cells. Hypoxic cytotoxicity ratio (HCR) was calculated as the intra-experiment quotient (oxic IC_{50})/(hypoxic IC_{50}). (b) Enhanced sensitivity to compounds in HR deficient cells. Hypersensitivity factor was determined by the intra-experiment quotient (IC_{50} $51D^{+/+}$)/(IC_{50} $51D^{-/-}$). Values are inter-experiment means and errors are SEM for 3–8 experiments. TPZ: tirapazamine; MECH: mechlorethamine; and CHL: chlorambucil.

nCBI, and 2-fold greater than TPZ, but lower than for TH-302 (Fig. 2a). As expected, the effector species for PR-104A and nCBI (PR-104H and aCBI, respectively), and the conventional nitrogen mustards chlorambucil and mechlorethamine were not selective for hypoxic cells. The latter observation suggests that HR was not significantly down-regulated by the short term (6 h) hypoxia used in these experiments, an interpretation supported by the lack of change in Rad51 by western blotting under these conditions (Supplementary Fig. S1). Interestingly, CEN-209 hypoxic selectivity was significantly lower in HR-deficient $51D^{-/-}$ cells compared to $51D^{+/+}$ cells (HCR 80 vs. 200, $P = 0.04$; Fig. 2a) suggesting distinct mechanisms of cytotoxicity under aerobic and hypoxic conditions.

The lower HCR for $51D^{-/-}$ cells appears to reflect a greater dependence on HR for resolution of oxic than hypoxic CEN-209 lesions, as shown by higher HF ratios under oxic conditions in Fig. 2b. A similar trend was observed for TPZ. Overall the DNA cross-linking HAPs were significantly more selective for HR-deficient cells than the benzotriazine di-*N*-oxides, with hypoxic HF of 26 and 17 for TH-302 and PR-104A, respectively. The aromatic nitrogen mustard active metabolite from PR-104A (PR-104H), the related DNA cross-linking agent chlorambucil and an analogue of the aliphatic mustard active metabolite from TH-302 (mechlorethamine) yielded HF values of a similar order (15–40). The DNA minor groove alkylating HAP nCBI was comparatively less selective for HR-deficient cells, although its active amino metabolite aCBI produced an HF of ~12.

3.3. DNA repair profile of the benzotriazine di-N-oxide prodrug class

To further investigate the repair of lesions induced by CEN-209 in oxic and hypoxic cells we generated DNA repair profiles for CEN-209, TPZ, the TPZ analogue CEN-309 [21] and chlorambucil by comparing sensitivity to these agents in CHO cells with loss-of-function mutations in the base excision repair (BER; Xrcc1), nucleotide excision repair (NER; Ercc1, Xpf, Ercc2), non-homologous end joining (NHEJ, Dna-pk), HR (Rad51d), and Fanconi anaemia (FA; FancG) pathways (Fig. 3). The full dataset for these experiments, which were performed independently of those illustrated in Fig. 2, is given in supplementary Table S2. This study confirmed the significantly greater dependence of CEN-209 cytotoxicity on Rad51d under oxic than hypoxic conditions ($P = 0.02$), and demonstrated distinct DNA repair profiles for CEN-209 under oxia and hypoxia across the cell line panel (Fig. 3) further supporting the existence of alternative mechanisms cytotoxicity. As compared with oxic lesions, hypoxic lesions induced by the benzotriazine di-*N*-oxides were less dependent on HR and BER and more dependent on NER genes. CEN-209 also demonstrated modest selectivity for V3 cells (*Prkdc* mutant) deficient in NHEJ as compared to AA8 wild type cells, but this was significant only under oxia ($P = 0.03$). These repair profiles were very similar in all three members of the benzotriazine di-*N*-oxide class. The DNA repair profiles for the di-*N*-oxides were clearly different from that of chlorambucil, which showed the classical dependence of a bifunctional alkylating agent on the NER, HR and FA pathways similar to that previously reported for PR-104A and PR-104H [9].

3.4. Relationships between metabolic reduction of CEN-209 and cytotoxicity

To explore further the apparent difference in DNA repair dependence of CEN-209 cytotoxicity under aerobic and hypoxic conditions, we utilised $51D^{+/+}$ and $51D^{-/-}$ cells in which one-electron reductase activity was increased by forced expression of soluble human NADPH:cytochrome P450 oxidoreductase (sPOR). Strong expression of sPOR was confirmed by Western blot (Fig. 4a) and provided a ~10-fold elevation in total POR reductase activity relative to control cells, as measured by rates of cyanide-resistant NADPH-dependent cytochrome c reduction (Fig. 4b). The POR activity of the parental and sPOR cell lines spanned the range observed in human tumour cell lines (Fig. 4b). In agreement with previous reports, POR expression conferred sensitivity to TPZ [46], PR-104A [50] and TH-302, but surprisingly did not significantly influence the cytotoxicity of nCBI (Fig. 4c). Notably, the potentiation of CEN-209 cytotoxicity by expression of sPOR was an order of magnitude greater in oxic cells (oxic IC_{50} ratio 160 vs. hypoxic ratio 17; $P = 0.04$), with a similar pattern for TPZ and TH-302, while the converse result was seen for PR-104A for which hypoxic cytotoxicity was enhanced more than oxic toxicity (Fig. 4c). The increase in oxic cytotoxicity of CEN-209 in cells with high POR

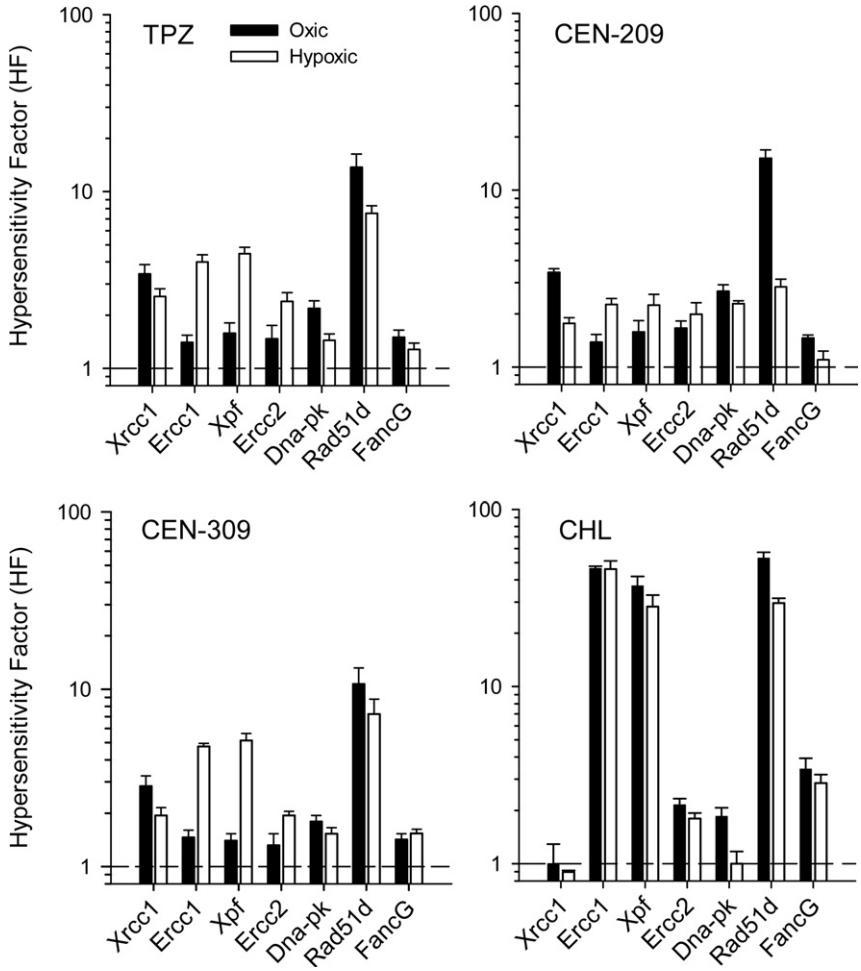

Fig. 3. DNA repair profile of benzotriazine di-*N*-oxide prodrugs (TPZ, CEN-209, CEN-309) compared with chlorambucil. CHO cells with loss-of-function mutations in the base excision repair (Xrcc1), nucleotide excision repair (Ercc1, Xpf, Ercc2), non-homologous end joining (Dna-pk), homologous recombination (Rad51d, cell line $51D^{-/-}$), and Fanconi anaemia (FancG) pathways were challenged with compounds in IC_{50} assays. Hypersensitivity factors (HFs) were determined by reference to isogenic repair competent cells as the intra-experiment quotient (IC_{50} repair competent)/(IC_{50} repair deficient) for each gas condition. Values are inter-experiment means and errors are SEM for 2–12 experiments.

activity led to a substantial loss of hypoxic selectivity in these cells (Fig. 5; $P = 0.04$). This same loss of hypoxic selectivity in the sPOR cells was also observed for TPZ and TH-302, and was independent of HR status (supplementary Table S1).

The finding that sPOR enhances oxic cytotoxicity of CEN-209 even more than its hypoxic cytotoxicity suggested that the relationship between reduction of the prodrug and cytotoxicity is different under the two conditions. To investigate this further, we quantified metabolic reduction of CEN-209 under the same conditions as the IC_{50} assays. There is currently no direct way to measure the cytotoxic metabolite(s) from CEN-209 reduction, which are presumed by analogy with TPZ [10,11] to be oxidising free radicals derived from the initial one-electron reduction product. We therefore assayed the more stable downstream 1-oxide and nor-oxide reduced metabolites of CEN-209 (see Fig. 8) by LC–MS/MS in $51D^{+/+}$ and $51D^{+/+}$ sPOR cells under oxia and hypoxia. This required use of lower cell densities for the sPOR line under hypoxia to avoid depletion of the prodrug under hypoxia (Fig. S2). Normalising for the cell density difference, hypoxic CEN-209 reduction was increased ~10-fold by sPOR expression (Fig. 6a). The 1-oxide and nor-oxide metabolites were also measurable in oxic cultures, although at lower concentrations, and again were increased (~50-fold) by sPOR expression (Fig. 6a). The CEN-209 concentration dependence of 1-oxide and nor-oxide formation was well fitted using a low affinity single site saturation model, enabling estimation of metabolite concentrations at equitoxic (IC_{50}) prodrug concentrations (Fig. 6b). Under hypoxia, there was no significant difference ($P = 0.25$) between the concentration of 1-oxide plus nor-oxide at IC_{50} for the high and low POR lines. However, under oxic conditions the concentration of the reduced metabolites at IC_{50} was higher than under hypoxia for $51D^{+/+}$, and was significantly lowered ($P < 0.001$) by sPOR expression (Fig. 6b). As discussed below, this observation is consistent with a contribution of redox cycling to oxic cytotoxicity of CEN-209 in cells with high one-electron reductase activity.

3.5. Redox cycling of CEN-209 in aerobic $51D^{+/+}$ sPOR cells

To determine whether CEN-209 redox cycles in aerobic cells with high one-electron reductase activity, we compared rates of rotenone-resistant oxygen consumption and H_2O_2 production in $51D^{+/+}$ and $51D^{+/+}$ sPOR cells exposed to CEN-209 (25–200 μM titration) in a polarographic respirometer adapted for simultaneously observing oxidation of the H_2O_2 fluorogenic probe Amplex UltraRed. CEN-209 elevated oxygen consumption in $51D^{+/+}$ sPOR cells, but not $51D^{+/+}$ cells, with some evidence of saturation kinetics at high concentration (Fig. 7a). Net H_2O_2 production also increased in POR over-expressing cells, with a sigmoidal dependence on CEN-209 concentration, and showed no increase in $51D^{+/+}$ cells (Fig. 7b). The non-linearity of ROS production with respect to

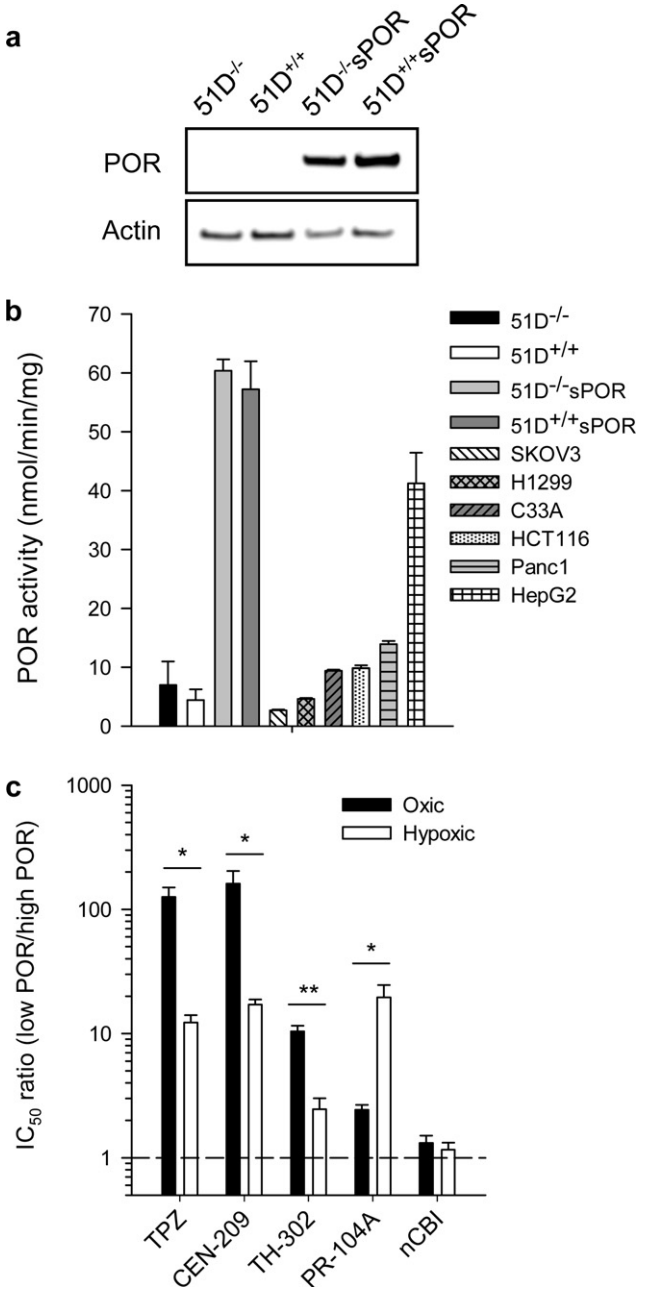

Fig. 4. The effect of sPOR expression on sensitivity of $51D^{+/+}$ cells to CEN-209 and reference prodrugs. (a) Confirmation of sPOR expression by Western blot. (b) POR activity measured as cyanide-resistant NADPH-dependent reduction of cytochrome c by spectrophotometric assay and compared to activity observed in commonly-used human tumour cell lines. (c) Relative sensitivity to HAPs in sPOR-expressing $51D^{+/+}$ cells compared to control $51D^{+/+}$ cells. The inter-experiment mean + SEM of the quotient (IC_{50} low POR)/(IC_{50} high POR) from $\geq$3 experiments is plotted.

oxygen consumption likely reflects the contribution of free radical scavenging and H_2O_2 catabolism at low CEN-209 concentration and depletion of Amplex UltraRed at high CEN-209 concentration. Together these data provide strong evidence for redox cycling of CEN-209 and generation of potentially cytotoxic ROS in aerobic cells with high POR reductase activity.

4. Discussion

We present here the first comprehensive comparison of the capacity for HAPs, representing four major chemical classes (benzotriazine di-*N*-oxides, dinitrobenzamide mustards, nitroimidazole mustards, and nitro-chloromethylbenzindolines), to exploit HR defects in hypoxic cells. Loss of Rad51d function, recently shown to confer susceptibility to ovarian carcinoma in humans [51], provides a severe HR phenotype that has been widely utilised as an informative pharmacodynamic model for examining the role of HR in chemosensitivity [9,27,52,53]. In this model we identify HAPs that generate DNA cross-linking metabolites (i.e. TH-302 and PR-104A) as the likely strongest candidates for exploiting HR defects; both prodrugs were markedly more active against $51D^{-/-}$ than $51D^{+/+}$ cells under anoxia (HF ratios 26 and 17 for TH-302 and PR-104A, respectively, which were not significantly different). Overall, TH-302 was 10 000$\times$ more active against hypoxic $51D^{-/-}$ cells than oxic $51D^{+/+}$ cells. In this respect it is interesting to note that TH-302 is currently undergoing phase II evaluation in pancreatic adenocarcinoma (NCT01144455), a malignancy to which germline mutation of the HR gene *PALB2* was recently reported to confer susceptibility [54]. The amino metabolite of nCBI was also selective for $51D^{-/-}$ cells, which is consistent with results for a related amino-CBI [52], although selectivity was diminished somewhat at the prodrug level.

The benzotriazine di-*N*-oxide class prodrugs – TPZ, CEN-209, CEN-309 – shared a broadly similar DNA repair profile that differed from that of the DNA cross-linking agent chlorambucil (Fig. 3) and reported profiles for PR-104A and PR-104H [9]. Under hypoxia the di-*N*-oxides were modestly selective for 51D1, EM9, UV4, UV41 and V3 cells which harbour mutations in *Rad51d*, *Xrcc1*, *Ercc1*, *Xpf* and *Prkdc*, respectively. UV4 and UV41 cells, which are deficient in NER (a pathway associated with several inherited cancer syndromes [55]), have been widely characterised as hypersensitive to bulky lesions including DNA cross-links [38], whereas EM9 cells are sensitive to single-strand breaks and base damage due to failure of DNA ligase III recruitment required for BER [36,56] and V3 cells are sensitive to agents that induce DNA double strand breaks repaired by NHEJ [42]. The absence of any one predominant repair pathway in the benzotriazine di-*N*-oxide hypoxic profiles is consistent with evidence for complex DNA damage in this class of agents, including base oxidation [57], DNA–protein adducts potentially involving topoisomerase II [27,58], and single- [12] and double-strand breaks [27,59].

The surprising finding of the present study that the DNA repair profile for CEN-209 (and other benzotriazine di-*N*-oxides) is different under oxic and hypoxic conditions suggests a qualitatively different spectrum of DNA lesions under the two conditions, with redox cycling identified as a potential mechanism of aerobic cytotoxicity, particularly in cells with high one-electron reductase activity. This result is consistent with earlier work describing redox cycling of TPZ in aerobic hepatocytes [60]. A model that describes relationships between bioreductive metabolism, redox chemistry, DNA damage and cytotoxicity of the benzotriazine di-*N*-oxides is proposed in Fig. 8, based on literature for TPZ and the present study. One-electron reduction by POR and other reductases (Fig. 8, reaction 1) generates an initial free radical that decays by reaction with O_2 (reaction 2, the basis for hypoxia-selective cytotoxicity), dismutation to the less toxic 1-oxide (reaction 3) or spontaneous fragmentation to an oxidising radical that was initially considered to be the hydroxyl radical [61] but for which accumulating evidence [10,62,63] implicates the benzotriazinyl radical (reaction 6). Superoxide formed by redox cycling in oxic cells (reactions 1 and 2) is metabolised to H_2O_2 by superoxide dismutases (reaction 7), potentially initiating Fenton-like formation of hydroxyl radical (reaction 9). DNA radicals generated by these oxidising radicals (reaction 10) are analogous to those from ionising radiation, the further oxidation of which by oxygen leads to DNA strand breaks (reaction 11). In hypoxic cells, this oxidation of DNA radicals is mediated by the benzotriazine-di-oxide prodrug itself or its 1-oxide

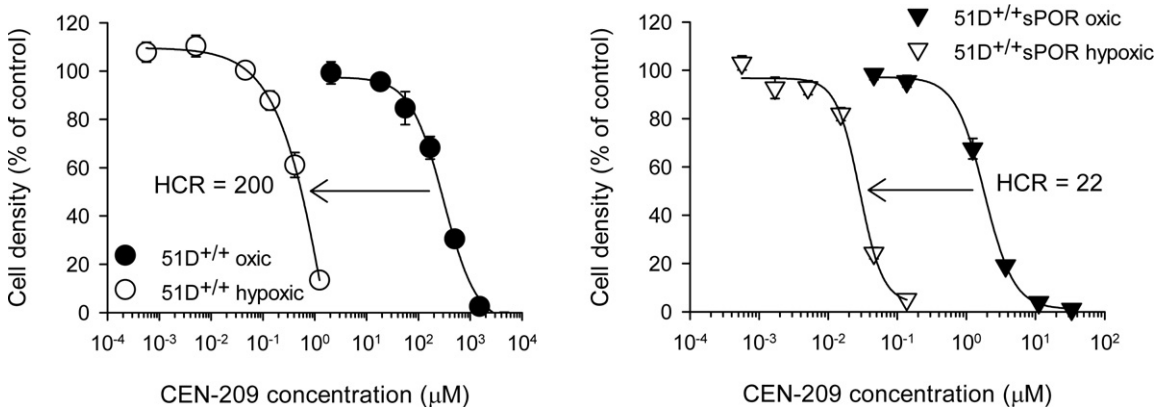

Fig. 5. Effect of sPOR expression on hypoxic selectivity of CEN-209. Data points show inter-experiment mean cell staining density + SEM of ≥3 IC_{50} experiments performed. Curves are four parameter logistic regressions. HCR values were calculated as the intra-experiment quotient (IC_{50} oxic)/(IC_{50} hypoxic) and are inter-experiment means.

metabolite [12,64,65]. The major cytotoxic lesions from TPZ under hypoxia show repair kinetics characteristic of multiply damaged sites from high LET radiation [59]; these complex lesions appear to arise from replication fork arrest (reaction 12) and depend on HR for their resolution [27] (reaction 15).

Our results for TPZ, CEN-209 and CEN-309 under hypoxia are consistent with the reported HR dependence of TPZ cytotoxicity under hypoxia, but the repair dependence of the oxic cytotoxicity of TPZ has not previously been described. The mechanism of oxic cytotoxicity of TPZ is in fact not well understood; the finding that cytotoxic potency is further suppressed as gas phase oxygen concentrations are increased above 20% O_2 [66,67] suggests that oxic cytotoxicity is due to incomplete suppression of the TPZ radical. However, other evidence suggests that oxic cytotoxicity is due to futile redox cycling, generating superoxide that can give rise to hydroxyl radicals via Fenton chemistry [68]. That high activity of a one-electron reductase (sPOR) enhances cytotoxicity of the benzotriazine di-*N*-oxides to a greater extent under oxia than hypoxia (Fig. 4c) confirms that the two mechanisms of cytotoxicity are distinctly different. Although the rate of the forward reaction of CEN-209 to its protonated radical (Fig. 8, reaction 1) is expected to be the same under oxic and acutely hypoxic conditions, and the ultimate cytotoxic radicals derive from the same di-*N*-oxide radical, under hypoxia the steady state concentration of the latter will be much higher and therefore the contribution of its second-order dismutation to the 1-oxide (Fig. 8, reaction 3) will be greater than under oxia. The latter detoxifying reaction may account for the smaller increase in hypoxic than oxic cytotoxicity when sPOR is expressed. The observations are therefore consistent with the redox cycling model of oxic cytotoxicity (i.e. that cell killing is dependent on superoxide and downstream ROS rather than the di-*N*-oxide radical).

The 1-oxide and nor-oxide metabolites of CEN-209 provide independent support for this model. Concentrations of these reduced metabolites were not significantly different for parental and sPOR-expressing cells at the CEN-209 concentrations corresponding to the hypoxic IC_{50}. At the aerobic IC_{50}, reduced metabolite concentrations for the parental line were higher than under hypoxia, which is opposite to the expected lower contribution of CEN-209 radical disproportionation and likely reflects a significant contribution from oxygen-insensitive two-electron reductases (Fig. 8, reaction 4) such as NAD(P)H:quinone oxidoreductase (DT-diaphorase). The latter is known to catalyse reduction of TPZ directly to its 1-oxide, bypassing the cytotoxic free radical

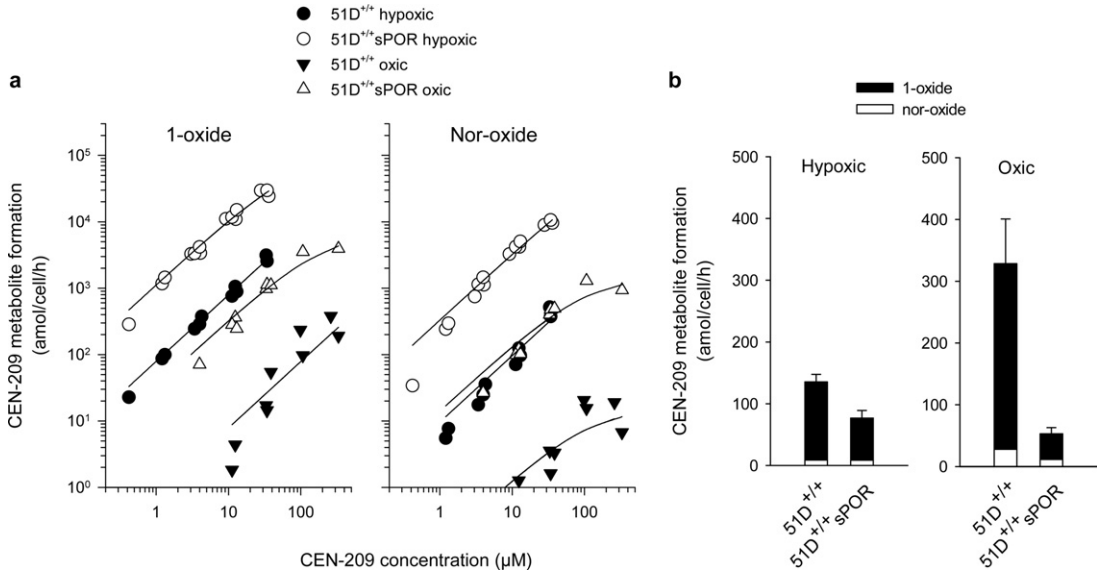

Fig. 6. Formation of reduced 1-oxide and nor-oxide metabolites of CEN-209 in $51D^{+/+}$ and $51D^{+/+}$ sPOR cultures under oxia and hypoxia by LC–MS/MS. (a) Rate of 1-oxide and nor-oxide formation normalised for cell density. Data were fitted using a single-site saturation model with 1/Y weighting. Values are pooled from 3 experiments. (b) Reduced metabolite formation (1-oxide plus nor-oxide) at CEN-209 IC_{50} concentration (1.5, 0.087, 280 and 1.9 μM for hypoxic $51D^{+/+}$, hypoxic $51D^{+/+}$ sPOR, oxic $51D^{+/+}$, and oxic $51D^{+/+}$ sPOR, respectively) by interpolation or extrapolation of the curves shown in (a). Values are mean and SEM (for sum of 1-oxide and nor-oxide) from 3 independent experiments.

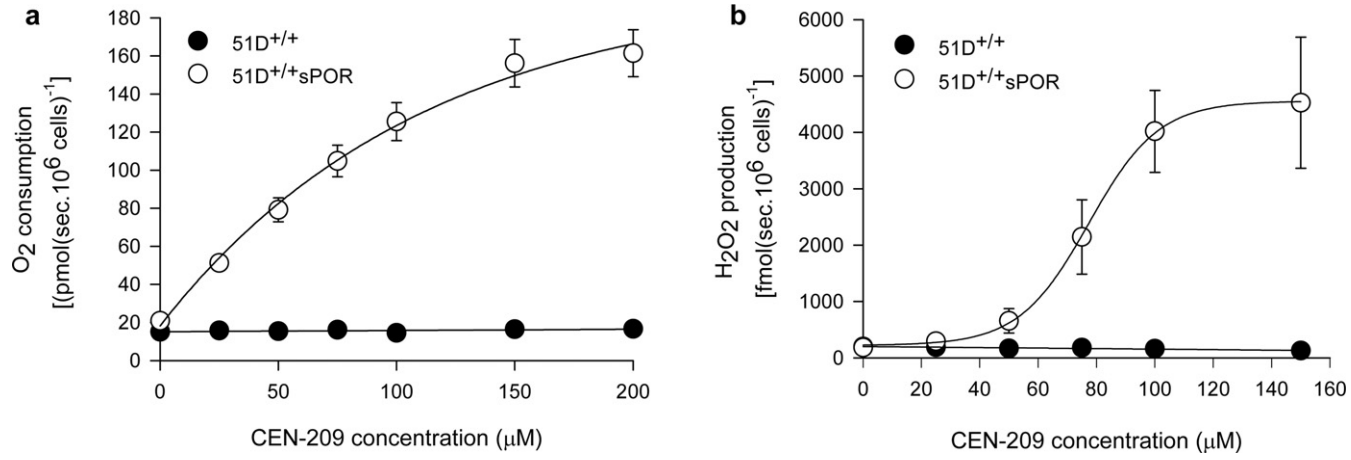

Fig. 7. Non-respiratory oxygen consumption and net H_2O_2 production in aerobic $51D^{+/+}$ and $51D^{+/+}$ sPOR cells exposed to CEN-209. Rate of rotenone-resistant oxygen consumption (a) and H_2O_2 production (b) in stirred $51D^{+/+}$ and $51D^{+/+}$ sPOR cell suspensions (5×10^5 cells/mL) as a function of CEN-209 concentration. CEN-209 was titrated to 200 μM and rates were defined as the steady-state flux achieved following each drug addition. Values are mean and SEM of 4 experiments performed for each cell line.

intermediate [69,70]. Notably, sPOR expression significantly lowered the 1-oxide plus nor-oxide concentration at the oxic IC_{50} (i.e. sPOR did not increase net reduction of CEN-209 as much as it increased cytotoxicity) which is consistent with enhanced redox cycling dominating the mechanism of cytotoxicity under oxic conditions in cells with high expression of one-electron reductases. The POR activity in the $51D^{+/+}$ sPOR line was at the top end of the range for human tumour cell lines we surveyed (Fig. 4b), suggesting that this redox-related cytotoxicity might contribute to cytotoxicity of CEN-209 in oxic cells in human tumours (and potentially normal tissues) with high one-electron reductase activity. It is unclear at present how redox cycling will contribute to CEN-209 cytotoxicity at intermediate pO_2, but may well play a part in killing the moderately hypoxic tumour cells that are probably the most important in resistance to fractionated radiotherapy [71].

Given the importance of template switching via HR for repair of complex DNA lesions [22], the greater dependence on HR for oxic than hypoxic cytotoxicity of benzotriazine di-*N*-oxides suggests the formation of lesions of higher complexity under aerobic conditions. This could reflect rapid inhibition of DNA synthesis as a result of dNTP pool depletion under severe hypoxia [72] (Fig. 8,

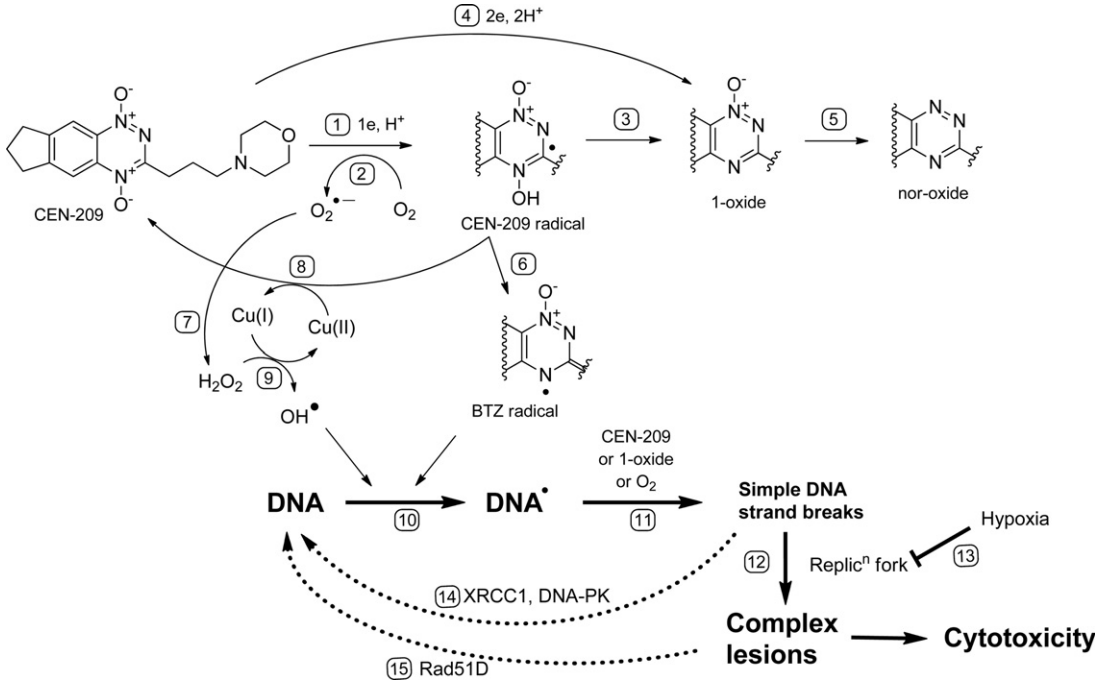

Fig. 8. Scheme showing proposed mechanism of action of CEN-209, based on results of the present study and analogy with tirapazamine. 1: One-electron reduction of CEN-209 (e.g. by POR). 2: Reoxidation of the CEN-209 radical by O_2, which is its primary mechanism of hypoxic selectivity. 3: Spontaneous dismutation to the 1-oxide metabolite. 4: Oxygen-insensitive two-electron reduction (e.g. by DT-diaphorase). 5: Further reduction to the nor-oxide. 6: Spontaneous formation of the oxidising benzotriazinyl radical. 7: Enzymatic (superoxide dismutase) and spontaneous dismutation of superoxide. 8: Reduction of Cu(II) by the CEN-209 radical. 9: Fenton-type reduction of H_2O_2 by Cu(I). 10: Oxidation of nucleobases and deoxyribose in DNA. 11: Further oxidation by oxygen (or CEN-209 and its 1-oxide under hypoxia) to generate frank DNA strand breaks. 12: Collision of replication forks with DNA damage, generating complex (cytotoxic) DNA lesions. 13: Replication fork arrest under severe hypoxia. 14: Repair of simple DNA breaks by BER and NHEJ pathways. 15: Repair of complex lesions by HR.

reaction 13), limiting collision of replication forks with damaged DNA (Fig. 8, reaction 12) which leads to stalled forks that depend on HR for their resolution [73]. Alternatively, initial oxidative damage to DNA may be more highly clustered under oxic than hypoxic conditions. If generated by redox cycling, superoxide dismutase and Fenton-type generation of hydroxyl radical from H_2O_2 (Fig. 8, reactions 2, 7, 9), low lesion complexity would normally be expected given that exogenously-administered H_2O_2 induces relatively non-cytotoxic (unclustered) single strand breaks in DNA [74]. However, the possibility of local hydroxyl radical generation from aerobic redox cycling of di-*N*-oxides is supported by observations that nuclear targeting of POR increased oxic rather than hypoxic cytotoxicity of TPZ in MDA-MB-231 cells, an effect that was reversed by treating with the copper chelator bathocuproine disulphonic acid (S. Jung, A. Tsai, D. Li, W.R. Wilson, A.V. Patterson unpublished observations). Copper ions have previously been implicated in the aerobic cytotoxicity of TPZ [75]. Clustered oxidative lesions could potentially arise through the local reduction of Cu(II) to Fenton-active Cu(I) by the TPZ radical [76] (Fig. 8, reaction 8), which will have restricted spatial distribution under oxic conditions because of its rapid reoxidation by O_2, in contrast to a more isotropic distribution in hypoxic cells. The nature of lesions induced by CEN-209 under aerobic and hypoxic conditions is a subject of ongoing investigation.

With several potential clinical assays for HR in development [77–79], this study provides a strong rationale for investigating use of HAPs of DNA-reactive cytotoxins for simultaneous targeting of hypoxia and HR defects in human cancer. HR may be exploitable both in tumours that frequently incur genetic or epigenetic derangements of the HR pathway, such as ovarian and triple-negative/*BRCA*-associated breast cancers, and secondary to microenvironmental suppression of HR in chronically hypoxic tumour cells. The latter approach was demonstrated recently using the poly(ADP-ribose) polymerase inhibitors ABT-888 and 4-amino-1,8-naphthalimide, which selectively killed hypoxic cells in xenografts presumably through a synthetic lethal interaction with suppression of HR [80]. Unlike PARP inhibitors, HAPs provide the major added advantage of hypoxia-selective release of the active HR-selective agent, thus limiting exposure in normal tissues.

The HAPs evaluated in the present study are all capable of exploiting HR defects as judged by their hyperactivity in *Rad51d* knockout cells, but the prodrugs that generate DNA interstrand cross-links under hypoxia (PR-104A and TH-302) show greater selectivity for this HR deficiency than the nCBI or benzotriazine di-*N*-oxide prodrugs. TH-302 showed the largest hypoxic selectivity, although, like the di-*N*-oxides, increasing POR activity stimulated aerobic more than hypoxic cytotoxicity of TH-302, unlike PR-104A where the converse was observed as previously reported [9]. Ultimately, the capacity for HAPs to exploit HR defects in clinical settings will depend not only on the nature of lesions generated but also on the exposure achievable at the site of action in hypoxic tissue, which will be a function of tolerability, systemic pharmacokinetics and extravascular drug transport in tumours. Moreover the available HAPs differ in the severity of hypoxia required for metabolic activation [3] so are likely to address different subpopulations of cells in tumours. Evaluation in preclinical tumour models is therefore needed to assist in identifying preferred prodrugs for exploiting microenvironmentally-induced down-regulation of HR in tumours.

Conflicts of interest

W.R. Wilson is an inventor on patents relating to PR-104A, and a shareholder and consultant to Proacta, Inc. M.P. Hay and W.R. Wilson are inventors on patents relating to CEN-209 and CEN-309, and consultants to Centella Therapeutics.

Acknowledgements

We thank Dr. Larry H. Thompson and Dr. Yongchuan Gu for provision of CHO cell lines, Dr. Moana Tercel for synthesis of nCBI and aCBI, Jiechuang Su for provision of S-9 fractions, and Dianne Ferry for synthesis of PR-104H. This research was supported by a Project Grant from the Health Research Council of New Zealand (10/459) and a Scholarship from the Genesis Oncology Trust (awarded to F.W. Hunter).

Appendix A. Supplementary data

Supplementary data associated with this article can be found, in the online version, at doi:10.1016/j.bcp.2011.12.005.

References

[1] Vaupel P, Hockel M, Mayer A. Detection and characterization of tumor hypoxia using pO_2 histography. Antioxid Redox Signal 2007;9:1221–35.
[2] Brown JM, Giaccia AJ. The unique physiology of solid tumors: opportunities (and problems) for cancer therapy. Cancer Res 1998;58:1408–16.
[3] Wilson WR, Hay MP. Targeting hypoxia in cancer therapy. Nat Rev Cancer 2011;11:393–410.
[4] Denny WA. Hypoxia-activated prodrugs in cancer therapy: progress to the clinic. Future Oncol 2010;6:419–28.
[5] Patterson AV, Ferry DM, Edmunds SJ, Gu Y, Singleton RS, Patel K, et al. Mechanism of action and preclinical antitumor activity of the novel hypoxia-activated DNA crosslinking agent PR-104. Clin Cancer Res 2007;13:3922–32.
[6] Duan JX, Jiao H, Kaizerman J, Stanton T, Evans JW, Lan L, et al. Potent and highly selective hypoxia-activated achiral phosphoramidate mustards as anticancer drugs. J Med Chem 2008;51:2412–20.
[7] Tercel M, Atwell GJ, Yang S, Ashoorzadeh A, Stevenson RJ, Botting KJ, et al. Selective treatment of hypoxic tumor cells in vivo: phosphate pre-prodrugs of nitro analogues of the duocarmycins. Angew Chem Int Ed 2011;50:2606–9.
[8] Singleton RS, Guise CP, Ferry DM, Pullen SM, Dorie MJ, Brown JM, et al. DNA crosslinks in human tumor cells exposed to the prodrug PR-104A: relationships to hypoxia, bioreductive metabolism and cytotoxicity. Cancer Res 2009;69:3884–91.
[9] Gu Y, Patterson AV, Atwell GJ, Chernikova SB, Brown JM, Thompson LH, et al. Roles of DNA repair and reductase activity in the cytotoxicity of the hypoxia-activated dinitrobenzamide mustard PR-104A. Mol Cancer Ther 2009;8:1714–23.
[10] Anderson RF, Shinde SS, Hay MP, Gamage SA, Denny WA. Activation of 3-amino-1,2,4-benzotriazine 1,4-dioxide antitumor agents to oxidizing species following their one-electron reduction. J Am Chem Soc 2003;125:748–56.
[11] Chowdhury G, Junnotula V, Daniels JS, Greenberg MM, Gates KS. DNA strand damage product analysis provides evidence that the tumor cell-specific cytotoxin tirapazamine produces hydroxyl radical and acts as a surrogate for O(2). J Am Chem Soc 2007;129:12870–7.
[12] Jones GD, Weinfeld M. Dual action of tirapazamine in the induction of DNA strand breaks. Cancer Res 1996;56:1584–90.
[13] Kotandeniya D, Ganley B, Gates KS. Oxidative DNA base damage by the antitumor agent 3-amino-1,2,4-benzotriazine 1,4-dioxide (tirapazamine). Bioorg Med Chem Lett 2002;12:2325.
[14] Shinde SS, Anderson RF, Hay MP, Gamage SA, Denny WA. Oxidation of 2-deoxyribose by benzotriazinyl radicals of antitumor 3-amino-1,2,4-benzotriazine 1,4-dioxides. J Am Chem Soc 2004;126:7865–74.
[15] von Pawel J, von Roemeling R, Gatzemeier U, Boyer M, Elisson LO, Clark P, et al. Tirapazamine plus cisplatin versus cisplatin in advanced non-small-cell lung cancer: a report of the international CATAPULT I study group. Cisplatin and tirapazamine in subjects with advanced previously untreated non-small-cell lung tumors. J Clin Oncol 2000;18:1351–9.
[16] Rischin D, Peters L, Fisher R, Macann A, Denham J, Poulsen M, et al. Tirapazamine, cisplatin, and radiation versus fluorouracil, cisplatin, and radiation in patients with locally advanced head and neck cancer: a randomized phase II trial of the Trans-Tasman Radiation Oncology Group (TROG 98.02). J Clin Oncol 2005;23:79–87.
[17] Rischin D, Peters LJ, O'Sullivan B, Giralt J, Fisher R, Yuen K, et al. Tirapazamine, cisplatin, and radiation versus cisplatin and radiation for advanced squamous cell carcinoma of the head and neck (TROG 02.02, HeadSTART): a phase III trial of the Trans-Tasman Radiation Oncology Group. J Clin Oncol 2010;28:2989–95.
[18] Rischin D, Hicks RJ, Fisher R, Binns D, Corry J, Porceddu S, et al. Prognostic significance of [18F]-misonidazole positron emission tomography-detected tumor hypoxia in patients with advanced head and neck cancer randomly assigned to chemoradiation with or without tirapazamine: a substudy of Trans-Tasman Radiation Oncology Group Study 98.02. J Clin Oncol 2006;24:2098–104.

[19] Peters LJ, O'Sullivan B, Giralt J, Fitzgerald TJ, Trotti A, Bernier J, et al. Critical impact of radiotherapy protocol compliance and quality in the treatment of advanced head and neck cancer: results from TROG 02.02. J Clin Oncol 2010;28:2996–3001.
[20] Hicks KO, Pruijn FB, Secomb TW, Hay MP, Hsu R, Brown JM, et al. Use of three-dimensional tissue cultures to model extravascular transport and predict in vivo activity of hypoxia-targeted anticancer drugs. J Natl Cancer Inst 2006;98:1118–28.
[21] Hicks KO, Siim BG, Jaiswal JK, Pruijn FB, Fraser AM, Patel R, et al. Pharmacokinetic/pharmacodynamic modeling identifies SN30000 and SN29751 as tirapazamine analogues with improved tissue penetration and hypoxic cell killing in tumors. Clin Cancer Res 2010;16:4946–57.
[22] Helleday T, Petermann E, Lundin C, Hodgson B, Sharma RA. DNA repair pathways as targets for cancer therapy. Nat Rev Cancer 2008;8:193–204.
[23] Evers B, Helleday T, Jonkers J. Targeting homologous recombination repair defects in cancer. Trends Pharmacol Sci 2010;31:372–80.
[24] Bindra RS, Schaffer PJ, Meng A, Woo J, Maseide K, Roth ME, et al. Down-regulation of Rad51 and decreased homologous recombination in hypoxic cancer cells. Mol Cell Biol 2004;24:8504–18.
[25] Chan N, Koritzinsky M, Zhao H, Bindra R, Glazer PM, Powell S, et al. Chronic hypoxia decreases synthesis of homologous recombination proteins to offset chemoresistance and radioresistance. Cancer Res 2008;68:605–14.
[26] Lu Y, Chu A, Turker MS, Glazer PM. Hypoxia-induced epigenetic regulation and silencing of the BRCA1 promoter. Mol Cell Biol 2011;31:3339–50.
[27] Evans JW, Chernikova SB, Kachnic LA, Banath JP, Sordet O, Delahoussaye YM, et al. Homologous recombination is the principal pathway for the repair of DNA damage induced by tirapazamine in mammalian cells. Cancer Res 2008;68:257–65.
[28] Hart CP, Meng F, Banica M, Evans J, Lan L, Lorente G, et al. In vitro activity profile of the novel hypoxia-activated cytotoxic prodrug TH-302. In: 99th AACR annual meeting; 2008 [abstract #1441].
[29] Boyd M, Hay MP, Boyd PD. Complete ^{1}H, ^{13}C and ^{15}N NMR assignment of tirapazamine and related 1,2,4-benzotriazine N-oxides. Magn Reson Chem 2006;44:948–54.
[30] Hay MP, Blaser A, Denny WA, Hicks KO, Lee HH, Pchalek K, et al. Tricyclic 1,2,4-triazine oxides and compositions therefrom for therapeutic use in cancer treatments. Patent EP1866292; 2010.
[31] Pchalek K, Hay MP. Stille coupling reactions in the synthesis of hypoxia-selective 3-alkyl-1,2,4-benzotriazine 1,4-dioxide anticancer agents. J Org Chem 2006;71:6530–5.
[32] Worrell JH, Jackman TA. Synthesis and characterization of cobalt(III) complexes derived from a pentadentate ligand having alkylamine and thioether donors to enhance stereospecificity. Inorg Chem 1978;17:3358–61.
[33] Denny WA, Atwell GJ, Yang S, Wilson WR, Patterson AV, Helsby NA. Novel nitrophenyl mustard and nitrophenylaziridine alcohols and their corresponding phosphates and their use as targeted cytotoxic agents. PCT/NZ 2004/529249; 2005.
[34] Thompson LH, Fong S, Brookman K. Validation of conditions for efficient detection of HPRT and APRT mutations in suspension-cultured Chinese hamster ovary cells. Mutat Res 1980;74:21–36.
[35] Hinz JM, Tebbs RS, Wilson PF, Nham PB, Salazar EP, Nagasawa H, et al. Repression of mutagenesis by Rad51D-mediated homologous recombination. Nucleic Acids Res 2006;34:1358–83.
[36] Thompson LH, Brookman KW, Dillehay LE, Carrano AV, Mazrimas JA, Mooney CL, et al. A CHO-cell strain having hypersensitivity to mutagens, a defect in DNA strand-break repair, and an extraordinary baseline frequency of sister-chromatid exchange. Mutat Res 1982;95:427–40.
[37] Busch DB, Cleaver JE, Glaser DA. Large-scale isolation of UV-sensitive clones of CHO cells. Somatic Cell Genet 1980;6:407–18.
[38] Hoy CA, Thompson LH, Mooney CL, Salazar EP. Defective DNA cross-link removal in Chinese hamster cell mutants hypersensitive to bifunctional alkylating agents. Cancer Res 1985;45:1737–43.
[39] Thompson LH, Busch DB, Brookman K, Mooney CL, Glaser DA. Genetic diversity of UV-sensitive DNA repair mutants of Chinese hamster ovary cells. Proc Natl Acad Sci USA 1981;78:3734–7.
[40] Brookman KW, Lamerdin JE, Thelen MP, Hwang M, Reardon JT, Sancar A, et al. (XPF) encodes a human nucleotide excision repair protein with eukaryotic recombination homologs. Mol Cell Biol 1996;16:6553–62.
[41] Thompson LH, Rubin JS, Cleaver JE, Whitmore GF, Brookman K. A screening method for isolating DNA repair-deficient mutants of CHO cells. Somatic Cell Genet 1980;6:391–405.
[42] Blunt T, Finnie NJ, Taccioli GE, Smith GC, Demengeot J, Gottlieb TM, et al. Defective DNA-dependent protein kinase activity is linked to V(D)J recombination and DNA repair defects associated with the murine scid mutation. Cell 1995;80:813–23.
[43] Tebbs RS, Hinz JM, Yamada NA, Wilson JB, Salazar EP, Thomas CB, et al. New insights into the Fanconi anemia pathway from an isogenic FancG hamster CHO mutant. DNA Repair (Amst) 2005;4:11–22.
[44] Hay MP, Gamage SA, Kovacs MS, Pruijn FB, Anderson RF, Patterson AV, et al. Structure-activity relationships of 1,2,4-benzotriazine 1,4-dioxides as hypoxia-selective analogues of tirapazamine. J Med Chem 2003;46:169–82.
[45] Skehan P, Storeng R, Scudiero D, Monks A, McMahon J, Vistica D, et al. New colorimetric cytotoxicity assay for anticancer-drug screening. J Natl Cancer Inst 1990;82:1107–12.
[46] Patterson AV, Saunders MP, Chinje EC, Talbot DC, Harris AL, Stratford IJ. Overexpression of human NADPH:cytochrome c (P450) reductase confers enhanced sensitivity to both tirapazamine (SR 4233) and RSU 1069. Br J Cancer 1997;76:1338–47.
[47] Wang J, Foehrenbacher A, Su J, Patel R, Hay MP, Hicks KO, et al. The 2-nitroimidazole EF5 is a biomarker for oxidoreductases that activate bioreductive prodrug CEN-209 under hypoxia. Clin Cancer Res; in press, doi:10.1158/1078-0432.CCR-11-2296.
[48] Hickey AJ, Renshaw GM, Speers-Roesch B, Richards JG, Wang Y, Farrell AP, et al. A radical approach to beating hypoxia: depressed free radical release from heart fibres of the hypoxia-tolerant epaulette shark (Hemiscyllum ocellatum). J Comp Physiol [B] 2011. doi: 10.1007/s00360-011-0599-6.
[49] Takata M, Sasaki MS, Sonoda E, Morrison C, Hashimoto M, Utsumi H, et al. Homologous recombination and non-homologous end-joining pathways of DNA double-strand break repair have overlapping roles in the maintenance of chromosomal integrity in vertebrate cells. EMBO J 1998;17:5497–508.
[50] Guise CP, Wang A, Thiel A, Bridewell D, Wilson WR, Patterson AV. Identification of human reductases that activate the dinitrobenzamide mustard prodrug PR-104A: a role for NADPH:cytochrome P450 oxidoreductase under hypoxia. Biochem Pharmacol 2007;74:810–20.
[51] Loveday C, Turnbull C, Ramsay E, Hughes D, Ruark E, Frankum JR, et al. Germline mutations in RAD51D confer susceptibility to ovarian cancer. Nat Genet 2011;43:879–82.
[52] Wilson WR, Stribbling SM, Pruijn FB, Syddall SP, Patterson AV, Liyanage HDS, et al. Nitro-chloromethylindolines: hypoxia-activated prodrugs of potent adenine *N*3 DNA minor groove alkylators. Mol Cancer Ther 2009;8:2903–13.
[53] Rajesh P, Litvinchuk AV, Pittman DL, Wyatt MD. The homologous recombination protein RAD51D mediates the processing of 6-thioguanine lesions downstream of mismatch repair. Mol Cancer Res 2011;9:206–14.
[54] Jones S, Hruban RH, Kamiyama M, Borges M, Zhang X, Parsons DW, et al. Exomic sequencing identifies PALB2 as a pancreatic cancer susceptibility gene. Science 2009;324:217.
[55] Cleaver JE, Lam ET, Revet I. Disorders of nucleotide excision repair: the genetic and molecular basis of heterogeneity. Nat Rev Genet 2009;10:756–68.
[56] Churchill ME, Peak JG, Peak MJ. Correlation between cell survival and DNA single-strand break repair proficiency in the Chinese hamster ovary cell lines AA8 and EM9 irradiated with 365-nm ultraviolet-A radiation. Photochem Photobiol 1991;53:229–36.
[57] Birincioglu M, Jaruga P, Chowdhury G, Rodriguez H, Dizdaroglu M, Gates KS. DNA base damage by the antitumor agent 3-amino-1,2,4-benzotriazine 1,4-dioxide (tirapazamine). J Am Chem Soc 2003;125:11607–15.
[58] Peters KB, Tirapazamine Brown JM. A hypoxia-activated topoisomerase II poison. Cancer Res 2002;62:5248–53.
[59] Wang J, Biedermann KA, Brown JM. Repair of DNA and chromosome breaks in cells exposed to SR 4233 under hypoxia or to ionizing radiation. Cancer Res 1992;52:4473–7.
[60] Silva JM, O'Brien PJ. Molecular mechanisms of SR 4233-induced hepatocyte toxicity under aerobic versus hypoxic conditions. Br J Cancer 1993;68:484–91.
[61] Daniels JS, Gates KS. DNA cleavage by the antitumor agent 3-amino-1,2,4-benzotriazine 1,4-dioxide (SR4233): evidence for involvement of hydroxyl radical. J Am Chem Soc 1996;118:3380–5.
[62] Shinde SS, Hay MP, Patterson AV, Denny WA, Anderson RF. Spin trapping of radicals other than the *OH radical upon reduction of the anticancer agent tirapazamine by cytochrome P450 reductase. J Am Chem Soc 2009;131:14220–1.
[63] Shinde SS, Maroz A, Hay MP, Patterson AV, Denny WA, Anderson RF. Characterization of radicals formed following enzymatic reduction of 3-substituted analogues of the hypoxia-selective cytotoxin 3-amino-1,2,4-benzotriazine 1,4-dioxide (tirapazamine). J Am Chem Soc 2010;132:2591–9.
[64] Hwang JT, Greenberg MM, Fuchs T, Gates KS. Reaction of the hypoxia-selective antitumor agent tirapazamine with a C1′-radical in single-stranded and double-stranded DNA: the drug and its metabolites can serve as surrogates for molecular oxygen in radical-mediated DNA damage reactions. Biochemistry (Mosc) 1999;38:14248–55.
[65] Siim BG, Pruijn FB, Sturman JR, Hogg A, Hay MP, Brown JM, et al. Selective potentiation of the hypoxic cytotoxicity of tirapazamine by its 1-N-oxide metabolite SR 4317. Cancer Res 2004;64:736–42.
[66] Koch CJ. Unusual oxygen concentration dependence of toxicity of SR-4233, a hypoxic cell toxin. Cancer Res 1993;53:3992–7.
[67] Hicks KO, Siim BG, Pruijn FB, Wilson WR. Oxygen dependence of the metabolic activation and cytotoxicity of tirapazamine: implications for extravascular transport and activity in tumors. Radiat Res 2004;161:656–66.
[68] Herscher LL, Krishna MC, Cook JA, Coleman CN, Biaglow JE, Tuttle SW, et al. Protection against SR 4233 (Tirapazamine) aerobic cytotoxicity by the metal chelators desferrioxamine and tiron. Int J Radiat Oncol Biol Phys 1994;30:879–85.
[69] Cahill A, Jenkins TC, White IN. Metabolism of 3-amino-1,2,4-benzotriazine-1,4-dioxide (SR 4233) by purified DT-diaphorase under aerobic and anaerobic conditions. Biochem Pharmacol 1993;45:321–9.
[70] Khan S, O'Brien PJ. Molecular mechanisms of tirapazamine (SR 4233, Win 59075)-induced hepatocyte toxicity under low oxygen concentrations. Br J Cancer 1995;71:780–5.
[71] Wouters BG, Brown JM. Cells at intermediate oxygen levels can be more important than the hypoxic fraction in determining tumor response to fractionated radiotherapy. Radiat Res 1997;147:541–50.
[72] Pires IM, Bencokova Z, Milani M, Folkes LK, Li JL, Stratford MR, et al. Effects of acute versus chronic hypoxia on DNA damage responses and genomic instability. Cancer Res 2010;70:925–35.
[73] Branzei D, Foiani M. Maintaining genome stability at the replication fork. Nat Rev Mol Cell Biol 2010;11:208–19.

[74] Olive PL, Johnston PJ. DNA damage from oxidants: influence of lesion complexity and chromatin organization. Oncol Res 1997;9:287–94.
[75] Lin PS, Ho KC. New cytotoxic mechanism of the bioreductive agent tirapazamine (SR 4233) mediated by forming complex with copper. Radiat Oncol Investig 1996;4:211–20.
[76] Wardman P. Electron transfer and oxidative stress as key factors in the design of drugs selectively active in hypoxia. Curr Med Chem 2001;8:739–61.
[77] Konstantinopoulos PA, Spentzos D, Karlan BY, Taniguchi T, Fountzilas E, Francoeur N, et al. Gene expression profile of BRCAness that correlates with responsiveness to chemotherapy and with outcome in patients with epithelial ovarian cancer. J Clin Oncol 2010;28:3555–61.
[78] Vollebergh MA, Lips EH, Nederlof PM, Wessels LF, Schmidt MK, van Beers EH, et al. An aCGH classifier derived from BRCA1-mutated breast cancer and benefit of high-dose platinum-based chemotherapy in HER2-negative breast cancer patients. Ann Oncol 2011;22:1561–70.
[79] Graeser M, McCarthy A, Lord CJ, Savage K, Hills M, Salter J, et al. A marker of homologous recombination predicts pathological complete response to neoadjuvant chemotherapy in primary breast cancer. Clin Cancer Res 2010;16:6159–68.
[80] Chan N, Pires IM, Bencokova Z, Coackley C, Luoto KR, Bhogal N, et al. Contextual synthetic lethality of cancer cell kill based on the tumor microenvironment. Cancer Res 2010;70:8045–54.